J Eng Math (2008) 61:201–217
DOI 10.1007/s10665-007-9151-9

Response of spatially tailored structures to thermal loading

Victor Birman · Ravinder Chona · Larry W. Byrd · Mark A. Haney

Received: 28 October 2006 / Accepted: 13 April 2007 / Published online: 29 June 2007
© Springer Science+Business Media B.V. 2007

Abstract The paper presents the formulation and analysis of composite plates serving as STATs, i.e., spatially tailored advanced thermal structures where the distribution of the constituent phases varies throughout the surface as well as through the thickness. This is an extension of the well-known concept of functionally graded materials (FGM) and structures with the constituent phases varying only in the latter direction. As a result of two- or three-dimensional grading it is possible to optimize the response and properties of the structure providing multitask and multi-scale optimization. The response of plates with two- or three-dimensional grading to an arbitrary thermal loading is elucidated, including the conditions that result in thermal bending versus thermal instability.

Keywords Composite plates · Functionally graded materials · Thermal buckling · Thermal stresses

1 Introduction

The concept of spatially tailored advanced thermal structures (STATs) is developed to address thermomechanical problems in aerospace and other applications. Typically, the goal is to optimize the response of the structure subject to a thermal field through an appropriate distribution of the material resulting in an optimum design. In particular, STATs may be useful in case of a nonuniform temperature distribution within the structure that is found in numerous aerospace applications as illustrated in the following paragraphs.

Consider for example, the temperature distribution in an aircraft panel that is in general three-dimensional and time-dependent regardless of the material used in the skin. The spatial variation occurs due to a variety of reasons, such as the convective heat-transfer coefficient or gas-temperature variations with position on either side of the panel. For hypersonic aircraft, catalytic effects caused by interaction of the plasma and the skin surface can cause large variations in the heat transfer to the surface. These effects can be very sensitive to the panel location on the aircraft. The thermal path into the substructure is also often different at different locations. A large spar with a high thermal conductivity provides a low resistance to energy transfer compared to natural convection. During heat-up, exposed

V. Birman (✉)
Engineering Education Center, University of Missouri-Rolla, One University Boulevard, St. Louis, MO 63121, USA
e-mail: vbirman@umr.edu

R. Chona · L. W. Byrd · M. A. Haney
Air Force Research Laboratory AFRL/VASM, Structural Sciences Center, Wright-Patterson Air Force Base, OH 45433, USA

panels may be on the order of 50°C cooler over a spar. Radiative heat transfer on either side of the panel also affects its temperature. The net amount of radiant energy exchange between two surfaces depends on the orientation and distance between the surfaces, so it is often nonuniform. Material properties are temperature-dependent which can affect the temperature gradient even for an isotropic material. The effect of temperature is even more pronounced on fiber-reinforced composite materials that have anisotropic thermal conductivity, as the energy is conducted along the fiber at a much higher rate than perpendicular to the fiber.

Transient conditions will also cause variations in temperature. For example, when an engine starts and hot exhaust gas impinges on a panel, the heated surface may be on the order of 100°C hotter than the back surface for a short period of time. Less pronounced effects occur when the engine speed is varied or the aircraft changes altitude or direction. The movement of a flap into or out of a hot gas stream changes its environment and thus its temperature.

All these effects lead to complex temperature distributions, even in the simplest panel constructed of a uniform isotropic skin supported on its edges. A spatially tailored aerothermal structure is specifically designed to produce the lightest system which can still carry the imposed mechanical loads, as well as survive the thermal environment.

Some of the advantages of conventional functionally graded materials are related to their ability to provide a better thermal protection and reduce delamination tendencies present in layered composites. In particular, in ceramic–metal systems these goals can be achieved by increasing the concentration of ceramic particles in the region adjacent to the heated surface using a heterogeneous single-layered structure. The unfortunate product of such design is asymmetry about the middle surface of the structure and bending–stretching coupling. As a result, displacements and stresses increase as compared to the symmetric counterpart of the same weight, while the buckling loads and natural frequencies decrease.

A comprehensive review of mechanics and applications of FGM that has recently been prepared [1] outlines studies on various structural configurations utilizing this concept. The following brief summary reflects on the recent research on thermal problems in FGM plates.

Previously published studies concerned with the response of FGM panels graded exclusively in the thickness direction include the analysis of thermal stresses in a thin FGM plate subjected to heat flux in the thickness direction by Tsukamoto [2]. The problems of transient thermal stresses in FGM rectangular plates due to a nonuniform (partial) heating have been considered by Ootao and Tanigawa [3]. They also published the exact solution for two-dimensional transient temperature and stress problems in a thick simply supported FGM strip subject to a heat flow as a result of suddenly applied nonuniform surface temperatures assuming that the strip is in the state of plane strain [4].

The asymptotic-expansion approach to heat conduction was employed by Reddy and Cheng to address three-dimensional thermoelastic problems in simply supported FGM plates subject to thermal or mechanical loading at one of the surfaces in [5]. The intriguing conclusion from this benchmark solution was that, while the standard assumption of a constant through the thickness deflection is acceptable in case of mechanical loading, it may become invalid if the load is thermal. Earlier investigations conducted by Reddy and his collaborators on static and dynamic thermomechanical problems in FGM plates appear in papers [6,7].

The exact solution of the thermomechanical three-dimensional problem of a simply supported shear-deformable rectangular FGM plate was presented by Vel and Batra [8,9] where the distribution of ceramic and metallic phases through the thickness was assumed to follow a power law for material volume fractions. The homogenization schemes employed in the paper included the Mori–Tanaka and self-consistent methods. Inertia forces were shown to have a negligible effect on deformations and stresses of thick FGM plates generated by transient thermal loads [10]. The nonlinear bending of geometrically nonlinear shear-deformable plates subject to thermal and/or mechanical loads was considered in [11] using a nonlinear version of the higher-order Reddy theory.

Thermal and mechanical buckling of rectangular plates was studied by Javaheri and Eslami [12] and [13]. Na and Kim used solid finite elements to investigate a three-dimensional thermal-buckling problem, though it should be noted that the sinusoidal and linear through-the-thickness temperature distributions in their study do not reflect the actual temperature distribution in a FGM plate [14]. The subsequent papers on the same subjects were recently published by these authors [15,16]; postbuckling was also considered in the latter article. Thermal buckling of simply supported skew plates subjected to temperature varying in the thickness direction was considered in [17]

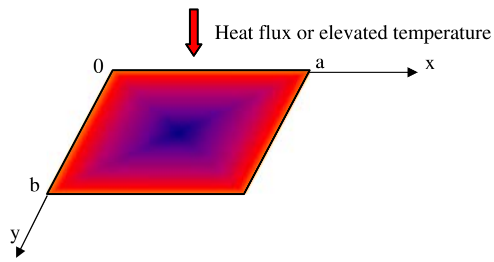

Fig. 1 Rectangular panel with in-plane grading (variations of grading are identified with different color intensity). The through-the-thickness grading (not shown) can also be variable

using a first-order shear deformation theory and the through-the-thickness temperature distribution obtained from the heat-conduction equation.

Other related studies, including dynamics of FGM plates in thermal fields and thermomechanical response of cylindrical shells are not included here (see for details, [1]). Contrary to the previously cited research concerned with the through-the-thickness graded plates, the present paper illustrates the comprehensive formulation of the problem and peculiarities introduced by a multidimensional (both in-plane and through-the-thickness) grading to the response of a panel subject to thermal loading. Note that a preliminary study for large-aspect ratio plates has recently been published by the authors [18].

2 Analysis

Consider a rectangular composite panel with an arbitrary grading of the constitutive phases that varies in the x-, y- and z-directions (Fig. 1). The panel is subject to thermal load (heat flux or elevated temperature) applied at one of the surfaces.

The comprehensive analysis of the problem requires the following steps:

(a) micromechanical characterization of the material yielding the properties and their distribution throughout the panel.
The review of various homogenization methods is included in the forthcoming paper [1]; it is assumed here that this task has been accomplished. Although the material is heterogeneous, it is considered point-wise isotropic in the subsequent analysis;
(b) the solution of the heat-transfer problem yielding the distribution of temperature throughout the panel.
This task that requires the analysis of a three-dimensional heat-conduction problem subject to thermal boundary conditions on the surfaces and along the edges is prohibitively complicated (although several problems have been solved for isotropic media). Accordingly, Mills suggested to solve similar problems numerically by a finite-element or finite-difference method, even in relatively simpler situations where the material is homogeneous [19, p. 131];
(c) formulation of the governing equations and boundary conditions necessary to solve bending, buckling and postbuckling problems.
This step is discussed in the following Sect. 2.1;
(d) characterization of the response of multidimensionally graded panels subject to thermomechanical loading (this is discussed in Sect. 2.2).

In addition, the paper illustrates the solution of several relevant problems. The Rayleigh–Ritz analysis of thermal bending of a simply supported panel with an arbitrary in-plane grading is considered in Sect. 2.3. The exact solution of the problem where a thin large-aspect-ratio panel is composed of strips of constant in-plane grading oriented along long edges is shown in Sect. 2.4. An example of the effect of boundary conditions on the response of a FGM plate graded in the thickness direction to in-plane uniform thermal loading is presented in Sect. 2.5. This elucidates the peculiarities of the effect of the boundary conditions on the response of thermally loaded structures. Finally, thermal stresses in a Ti/TiB (titanium/titanium boride) plate with initial imperfections obtained by ABAQUS are shown for various grading schemes in Sect. 2.6. As follows from the latter example, using functionally through-the-thickness graded materials and/or multidimensional piece-wise grading can be an effective tool for optimizing the response of the panel.

2.1 Governing equations

The analysis is conducted by the thin-plate theory, the corresponding assumptions being omitted for brevity. The vectors of the stress, stress resultants and stress couples at an arbitrary location are given by

$$\{\vec{\sigma}\} = [Q]\{\vec{\varepsilon} - \vec{\alpha}T\}, \quad \left(\vec{N}, \vec{M}\right) = \int_{-h/2}^{h/2} [Q]\{\vec{\varepsilon} - \vec{\alpha}T\}(1, z)\,\mathrm{d}z, \tag{1}$$

where the integration is conducted over the thickness of the panel h. The matrix of reduced stiffness, the vector of the coefficients of thermal expansion and the strain–displacement relationships are shown for a point-wise isotropic heterogeneous panel using standard notation

$$[Q] = \begin{bmatrix} Q_{11}(x,y,z) & Q_{12}(x,y,z) & 0 \\ Q_{12}(x,y,z) & Q_{11}(x,y,z) & 0 \\ 0 & 0 & Q_{66}(x,y,z) \end{bmatrix}, \quad \{\vec{\alpha}\} = \begin{Bmatrix} \alpha(x,y,z) \\ \alpha(x,y,z) \\ 0 \end{Bmatrix},$$

$$\{\vec{\varepsilon}\} = \begin{Bmatrix} \varepsilon_x^0 + z\kappa_x \\ \varepsilon_y^0 + z\kappa_y \\ \gamma_{xy}^0 + z\kappa_{xy} \end{Bmatrix} = \begin{Bmatrix} u,_x + \underline{\tfrac{1}{2}w,_x^2} - zw,_{xx} \\ v,_y + \underline{\tfrac{1}{2}w,_y^2} - zw,_{yy} \\ u,_y + v,_x + \underline{w,_{xy}^2} - 2zw,_{xy} \end{Bmatrix}. \tag{2}$$

The underlined nonlinear terms are omitted if the deformations are small (geometrically linear problem).

The substitution of (2) in (1) yields the expressions for stress resultants and stress couples shown here for a linear problem:

$$\begin{Bmatrix} N_x \\ N_y \\ N_{xy} \end{Bmatrix} = \begin{bmatrix} A_{11}(x,y) & A_{12}(x,y) & 0 \\ A_{12}(x,y) & A_{11}(x,y) & 0 \\ 0 & 0 & A_{66}(x,y) \end{bmatrix} \begin{Bmatrix} u,_x \\ v,_y \\ u,_y + v,_x \end{Bmatrix}$$
$$- \begin{bmatrix} B_{11}(x,y) & B_{12}(x,y) & 0 \\ B_{12}(x,y) & B_{11}(x,y) & 0 \\ 0 & 0 & B_{66}(x,y) \end{bmatrix} \begin{Bmatrix} w,_{xx} \\ w,_{yy} \\ 2w,_{xy} \end{Bmatrix} - \begin{Bmatrix} N_x^T \\ N_y^T \\ 0 \end{Bmatrix},$$

$$\begin{Bmatrix} M_x \\ M_y \\ M_{xy} \end{Bmatrix} = \begin{bmatrix} B_{11}(x,y) & B_{12}(x,y) & 0 \\ B_{12}(x,y) & B_{11}(x,y) & 0 \\ 0 & 0 & B_{66}(x,y) \end{bmatrix} \begin{Bmatrix} u,_x \\ v,_y \\ u,_y + v,_x \end{Bmatrix}$$
$$- \begin{bmatrix} D_{11}(x,y) & D_{12}(x,y) & 0 \\ D_{12}(x,y) & D_{11}(x,y) & 0 \\ 0 & 0 & D_{66}(x,y) \end{bmatrix} \begin{Bmatrix} w,_{xx} \\ w,_{yy} \\ 2w,_{xy} \end{Bmatrix} - \begin{Bmatrix} M_x^T \\ M_y^T \\ 0 \end{Bmatrix}, \tag{3}$$

where the stiffness terms and thermal contributions are

$$\left\langle A_{ij}(x,y), B_{ij}(x,y), D_{ij}(x,y)\right\rangle = \int_{-h/2}^{h/2} Q_{ij}(x,y,z)\left\langle 1, z, z^2\right\rangle \mathrm{d}z,$$

$$\left\langle \vec{N}^T(x,y), \vec{M}^T(x,y)\right\rangle = \int_{-h/2}^{h/2} [Q(x,y,z)]\{\vec{\alpha}(x,y,z)\}\,T(x,y,z)\,\langle 1, z\rangle\,\mathrm{d}z. \tag{4}$$

The equilibrium equations of a panel in terms of stress resultants and stress couples do not depend on a particular material or its grading:

$$N_x,_x + N_{xy},_y = 0, \; N_{xy},_x + N_y,_y = 0, \tag{5}$$
$$M_x,_{xx} + 2M_{xy},_{xy} + M_y,_{yy} + N_x w,_{xx} + 2N_{xy} w,_{xy} + N_y w,_{yy} = 0.$$

As long as the bending problem is geometrically linear, the stress resultants in the last of Eq. 5 do not account for the effect of deformations, i.e.,

$$N_x \to -N_x^T, \quad N_y \to -N_y^T, \; N_{xy} \to 0.$$

Contrary to conventional structures without in-plane grading of constituent phases, the equilibrium equations in terms of displacements available from (5) and (3) include derivatives of the elements of the stiffness matrices $[A], [B]$ and $[D]$. Accordingly, the integration of such equations appears impractical, except for special cases. Representing the governing equations in terms of the deflection w and the stress function does not simplify the analysis for the same reason. Nevertheless, qualitative conclusions regarding the character of the response of the panel that are discussed below are available from the analysis of (5) and the boundary conditions.

The solution must satisfy the boundary conditions; the four conditions that must be satisfied at every edge of the panel are (the case of elastic support in not included):

$$\begin{array}{llll}
x = 0, x = a: & u = 0 & \text{or} & N_x = 0, \\
 & v = 0 & \text{or} & N_{xy} = 0, \\
 & w = 0 & \text{or} & M_x,_x + 2M_{xy},_y + N_x w,_x + N_{xy} w,_y = 0, \\
 & w,_x = 0 & \text{or} & M_x = 0; \\
y = 0, y = b: & v = 0 & \text{or} & N_y = 0, \\
 & u = 0 & \text{or} & N_{xy} = 0, \\
 & w = 0 & \text{or} & M_y,_y + 2M_{xy},_x + N_y w,_y + N_{xy} w,_x = 0, \\
 & w,_y = 0 & \text{or} & M_y = 0.
\end{array} \tag{6}$$

The static conditions in (6) that include the stress resultants N_x, N_y and the stress couples M_x, M_y are nonhomogeneous due to the presence of thermal terms. The Kirchhoff conditions $M_i,_i + 2M_{ij},_j + N_i w,_i + N_{ij} w,_j = 0$ associated with free edges [20] are homogeneous only if the temperature in the panel is uniform.

Two types of response that are distinguished in the subsequent discussion are:

(1) Bending in response to an increasing thermal loading without "classical" thermal buckling;
(2) Buckling without prebuckling bending, i.e., prebuckling deformations are limited to the plane of the panel.

As is easy to observe from the equilibrium equations and the boundary conditions, bending is unavoidable if these equations are nonhomogeneous with respect to displacements. However, if the governing equations in terms of the displacements are homogeneous, the panel subject to thermal loading experiences only in-plane deformations followed by buckling.

It is noted that, as long as the temperature in the panel is a variable function of the in-plane coordinates, Eqs. 5 are nonhomogeneous due to terms such as $N_x^T,_x$, $N_y^T,_y$, $M_x^T,_{xx}$ and $M_y^T,_{yy}$. This means that the panel will experience bending deformations if it is subject to heating resulting in a temperature that is a function which is differentiable with respect to the in-plane coordinates (Fig. 2a). However, this primary bending state may become unstable resulting in instability (in flat panels such instability is associated with an alternative load-deformation path, rather than catastrophic snap-through buckling typical for shells). The instability analysis is based on finding the loading conditions corresponding to a nontrivial solution of the linearized variational equilibrium equations subject to linearized variational boundary conditions. Postbuckling behavior requires the solution of a geometrically nonlinear problem that is not considered in this paper. Whether the panel buckles and switches to an alternative postbuckling path or remains stable, the ultimate failure is due to the loss of strength.

The variations of the vectors of stress resultants and stress couples that occur at a specified load are

$$\left\{ \begin{array}{c} \delta \vec{N} \\ \delta \vec{M} \end{array} \right\} = \left[\begin{array}{cc} A(x, y) & B(x, y) \\ B(x, y) & D(x, y) \end{array} \right] \left\{ \begin{array}{c} \delta \vec{\varepsilon}^0 \\ \delta \vec{\kappa} \end{array} \right\}, \tag{7}$$

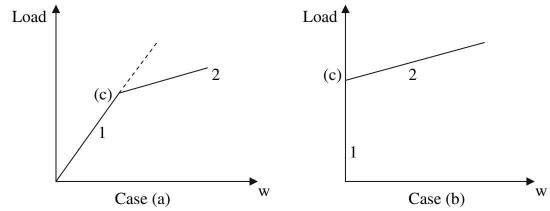

Fig. 2 Two types of the response of panels to thermal loading. Case (a): Primary bending path (1) becomes unstable at a critical load (c). Subsequently, the panel follows the postbuckling path (2). Case (b): Prebuckling deformations (1) are limited to the in-plane displacements (without bending). Upon buckling, the panel follows the postbuckling path (2)

where the matrices of extensional, coupling and bending stiffness are defined in (4), while the vectors of the variations of mid-plane strains and changes of curvature and twist are

$$\begin{aligned} \delta\vec{\varepsilon}^0 &= \left\{ \begin{array}{l} \delta u,_x + \underline{w,_x \delta w,_x} + \underline{\underline{\tfrac{1}{2}\delta w,_x^2}} \\ \delta v,_y + \underline{w,_y \delta w,_y} + \underline{\underline{\tfrac{1}{2}\delta w,_y^2}} \\ \delta u,_y + \delta v,_x + \underline{2w,_{xy} \delta w,_{xy}} + \underline{\underline{\delta w,_{xy}^2}} \end{array} \right\}, \\ \delta\vec{\kappa} &= -\left\{ \delta w,_{xx} \quad \delta w,_{yy} \quad 2\delta w,_{xy} \right\}^T. \end{aligned} \tag{8}$$

The singly underlined terms in (8) should be incorporated in the stability analysis of the primary bending state if it is desirable to account for the effect of prebuckling deformations on stability. Both doubly underlined terms as well as the singly underlined ones should be retained in the postbuckling analysis of the panel.

The variational equations of equilibrium are represented by

$$\begin{aligned} &\delta N_x,_x + \delta N_{xy},_y = 0, \quad \delta N_{xy},_x + \delta N_y,_y = 0, \\ &\delta M_x,_{xx} + 2\delta M_{xy},_{xy} + \delta M_y,_{yy} + N_x \delta w,_{xx} + 2N_{xy}\delta w,_{xy} + N_y \delta w,_{yy} \\ &\quad + \delta N_x w,_{xx} + 2\delta N_{xy} w,_{xy} + \delta N_y w,_{yy} = 0. \end{aligned} \tag{9}$$

The variational form of the boundary conditions is

$$\begin{array}{llll} x=0, x=a: & \delta u = 0 & \text{or} & \delta N_x = 0, \\ & \delta v = 0 & \text{or} & \delta N_{xy} = 0, \\ & \delta w = 0 & \text{or} & \delta M_x,_x + 2\delta M_{xy},_y + N_x \delta w,_x + \delta N_x w,_x + N_{xy}\delta w,_y + \delta N_{xy} w,_y = 0, \\ & \delta w,_x = 0 & \text{or} & \delta M_x = 0; \\ y=0, y=b: & \delta v = 0 & \text{or} & \delta N_y = 0, \\ & \delta u = 0 & \text{or} & \delta N_{xy} = 0, \\ & \delta w = 0 & \text{or} & \delta M_y,_y + 2\delta M_{xy},_x + N_y \delta w,_y + \delta N_y w,_y + N_{xy}\delta w,_x + \delta N_{xy} w,_x = 0, \\ & \delta w,_y = 0 & \text{or} & \delta M_y = 0. \end{array} \tag{10}$$

It is easy to check that both the linearized variational equilibrium equations as well as all possible combinations of linearized variational boundary conditions are homogeneous with respect to variations of the displacements δu, δv and δw. This means that the bending solution becomes unstable at a critical thermal load (if the panel does not collapse prior to achieving this load due to a loss of strength).

2.2 Characterization of the response dependent on the grading of the panel

Several grading scenarios are considered in this section to arrive at general conclusions about the anticipated response of a panel subject to thermal loading. The discussion is based on the governing equations considered in the previous section.

2.2.1 Case 1: In-plane grading is an arbitrary continuous function of in-plane coordinates

In this case the properties of the material of the panel are also continuous functions of the in-plane coordinates. The temperature distribution varies throughout the panel, being dependent on the thickness coordinate but, more important for this discussion, also varying in the x- and y-directions, irrespective of the mode of application of the thermal load. Accordingly, thermal contributions to the stress resultants and couples are differentiable functions of the in-plane coordinates. This implies that the equilibrium equations (5) and the static boundary conditions in (6) are nonhomogeneous. As a result, the panel experiences bending deformations until it fails due to the loss of strength or becomes unstable at the critical thermal load obtained from the variational equations (9) and (10).

The only exception from this type of response is an unlikely case where thermal stress couples and stress resultants are constant throughout the panel. Then the thermal terms are present but their derivatives with respect to the in-plane coordinates are equal to zero. Therefore, a panel with an arbitrary grading may buckle without developing prebuckling bending deformations as shown in Fig. 2b if the boundary conditions are

$$\begin{aligned} &x = 0, x = a : u = w,_x = 0, v = 0 \text{ or } N_{xy} = 0, w = 0 \text{ or } M_x,_x + 2M_{xy},_y + N_x w,_x + N_{xy} w,_y = 0, \\ &y = 0, y = b : v = w,_y = 0, u = 0 \text{ or } N_{xy} = 0, w = 0 \text{ or } M_y,_y + 2M_{xy},_x + N_y w,_y + N_{xy} w,_x = 0. \end{aligned} \tag{11}$$

Note that, although the terms $N_x w,_x$ and $N_y w,_y$ include thermal contributions, the boundary conditions remain homogeneous, i.e., prebuckling bending does not occur.

2.2.2 Case 2: Piece-wise in-plane grading

Let the volume fractions of the constituent phases of the panel be represented as $V_c(x, y, z) = V_{cx}(x)\, V_{cy}(y)\, V_{cz}(z)$, where c denotes a constituent material phase. Furthermore, the panel is subdivided into regions $x_i \le x \le x_{i+1}$, $y_j \le y \le y_{j+1}$, such that it is graded only in the thickness direction within each region. Accordingly,

$$V_c(x, y, z) = \sum_{ij} V_{cij}(z)\, \delta_{ij}, \tag{12}$$

where $V_{cij}(z)$ are functions that are independent of x and y and

$$\begin{aligned} &\delta_{ij} = 1 \quad \text{if } x_i \le x \le x_{i+1}, y_j \le y \le y_{j+1}, \\ &\delta_{ij} = 0 \text{ otherwise.} \end{aligned} \tag{13}$$

The result of such grading is an abrupt change in the heat-conduction coefficient across the boundaries of the regions, i.e., across $x = x_i$, $x = x_{i+1}$, $y = y_j$, $y = y_{j+1}$. As a consequence, heat conduction takes place across these boundaries and while the temperature may predominantly be a function of the z-coordinate within the corresponding panel region, it is impossible to disregard the temperature variations in the x-direction across the boundaries $x = x_i$, $x = x_{i+1}$ and the temperature variations in the y-direction across $y = y_j$, $y = y_{j+1}$. This implies the presence of non-negligible derivatives $N_x^T,_x$ and $N_y^T,_y$ across the respective boundaries, although they become small in the interior of the corresponding region. The thermal contributions $M_x^T,_{xx}$ and $M_y^T,_{yy}$ are also present across the region boundaries, except for the situation where the second derivatives of the temperature are equal to zero. As a result, the governing and static boundary conditions are nonhomogeneous and the panel experiences bending that increases with increasing thermal load.

If the panel subject to a uniform temperature is very thin, the heat flow across the regions of piece-wise in-plane constant grading may be negligible due to convection and radiation from the surfaces. In this case, the nonhomogeneous terms in the equilibrium equations and the boundary conditions may become negligible as well and prebuckling bending may be disregarded. Accordingly, buckling may closely approximate the response mode for such panels.

2.2.3 Case 3: Grading in the thickness direction only

As was discussed above, the only situation where prebuckling bending deformations do not occur in panels with in-plane grading is the case where thermal stress couples and stress resultants are constant and the boundary conditions correspond to (11). If the panel is graded in the thickness direction only but the applied thermal load is nonuniform, i.e., the temperature or heat flux applied at the surface depend on the in-plane coordinates, bending is unavoidable due to nonzero thermal terms in the equilibrium equations and the static boundary conditions.

Consider now a particular situation where the thermal load is uniform over the surface of the panel and $V_c = V_c(z)$. Then the heat flow occurs only in the thickness direction and $T = T(z)$. Accordingly, the derivatives of the thermal terms in (5) are equal to zero, i.e., the equilibrium equations are homogeneous. Nevertheless, the thermal terms that appear in the boundary conditions make the problem nonhomogeneous, except for the case where the boundary conditions are given by (11). Moreover, as will be shown below, the boundary condition for a large-aspect-ratio panel with long edges that are not restrained against out-of-plane displacements, i.e., $N_x(x = 0, x = a) = 0$, are homogeneous and prebuckling deformations occur only in the plane of the panel (see Sect. 2.5).

Therefore, clamped panels with numerous types of in-plane boundary conditions do not develop prebuckling bending deformations and their response mode can be identified with buckling followed by a stable postbuckling deformation path (Fig. 2b). It is emphasized that such a response is impossible in panels with an in-plane grading subject to a uniform-over-the-surface thermal load due to heat flow in the x- and y-directions that results in a nonuniform temperature within the panel.

Note that, although almost all studies of FGM panels subjected to a uniform heat flow or surface temperature assume that the temperature in the panel varies only in the thickness direction, a high thermal conductivity of supporting boundary elements (spars, bulkheads or frames) implies that $T = T(x, y)$. Hence the discussion on the cases where prebuckling deformations occur in the plane of the plate prior to buckling refers to a rather theoretical situation.

2.3 A Rayleigh–Ritz bending analysis of a simply supported panel with arbitrary in-plane grading

This section illustrates the analytical solution for the case where in-plane grading is arbitrary. The Rayleigh–Ritz solution is a useful approach if the in-plane distributions of volume fractions of the constituent materials, i.e., $V_{cx}(x)$ and $V_{cy}(y)$, are continuous analytical functions of the corresponding coordinates so that an exact integration of the equilibrium equations is prohibitively complicated or impossible.

The potential energy of a point-wise isotropic FGM panel that is arbitrarily graded both in-plane as well as in the thickness direction is given by

$$\begin{aligned}\Pi =\ & \frac{1}{2}\int_0^a\int_0^b\int_{-h/2}^{h/2}\left[\sigma_x(\varepsilon_x - \alpha T) + \sigma_y\left(\varepsilon_y - \alpha T\right) + \tau_{xy}\gamma_{xy}\right]\mathrm{d}z\,\mathrm{d}y\,\mathrm{d}x \\ & + \frac{1}{2}\int_0^a\int_0^b\left(N_x w,_x^2 + 2N_{xy}w,_x w,_y + N_y w,_y^2\right)\mathrm{d}y\,\mathrm{d}x \end{aligned} \tag{14}$$

The substitution of the expressions for the stresses and strains (1), (2) in (14) and the integration throughout the thickness of the panel yields

$$\begin{aligned}\Pi = \frac{1}{2}\int_0^a\int_0^b & [A_{11}u,_x^2 - 2B_{11}u,_x w,_{xx} + D_{11}w,_{xx}^2 + 2A_{12}u,_x v,_y - 2B_{12}(v,_y w,_{xx} + u,_x w,_{yy}) + 2D_{12}w,_{xx} w,_{yy} \\ & + A_{22}v,_y^2 - 2B_{22}v,_y w,_{yy} + D_{22}w,_{yy}^2 + A_{66}(u,_y + v,_x)^2 - 4B_{66}(u,_y + v,_x)w,_{xy} + 4D_{66}w,_{xy}^2 - 2N_x^T u,_x \\ & - 2N_y^T v,_y + 2M_x^T w,_{xx} + 2M_y^T w,_{yy}]\mathrm{d}y\,\mathrm{d}x - \frac{1}{2}\int_0^a\int_0^b\left(N_x^T w,_x^2 + N_y^T w,_y^2\right)\mathrm{d}y\,\mathrm{d}x, \end{aligned} \tag{15}$$

where $A_{ij} = A_{ij}(x, y)$, $B_{ij} = B_{ij}(x, y)$, $D_{ij} = D_{ij}(x, y)$, $M_i^T = M_i^T(x, y)$, $N_i^T = N_i^T(x, y)$. The higher-order terms are omitted in (15).

It should be noted that Eq. (15) could be also obtained from [21]. However, contrary to the class of problems considered in [21], the present formulation is more complex, including stiffness and thermal terms dependent on the in-plane coordinates.

Consider a panel that is simply supported along all edges by frames or bulkheads, each of them infinitely stiff within its plane. In practical situations supporting structures can usually be modeled using such restrictions. The corresponding boundary conditions are

$$x = 0, \quad x = a : v = w = 0; \quad y = 0, \quad y = b : u = w = 0. \tag{16a}$$

The out-of-plane and torsional stiffness of supports is often negligible, so that conditions (16a) are complemented by

$$\begin{aligned} &x = 0, \ x = a: \\ &\qquad N_x = A_{11}(x, y)\, u_{,x} + A_{12}(x, y)\, v_{,y} - B_{11}(x, y)\, w_{,xx} - B_{12}(x, y)\, w_{,yy} - N_x^T = 0, \\ &\qquad M_x = B_{11}(x, y)\, u_{,x} + B_{12}(x, y)\, v_{,y} - D_{11}(x, y)\, w_{,xx} - D_{12}(x, y)\, w_{,yy} - M_x^T = 0; \\ &y = 0, \ y = b: \\ &\qquad N_y = A_{12}(x, y)\, u_{,x} + A_{22}(x, y)\, v_{,y} - B_{12}(x, y)\, w_{,xx} - B_{22}(x, y)\, w_{,yy} - N_y^T = 0, \\ &\qquad M_y = B_{12}(x, y)\, u_{,x} + B_{22}(x, y)\, v_{,y} - D_{12}(x, y)\, w_{,xx} - D_{22}(x, y)\, w_{,yy} - M_y^T = 0. \end{aligned} \tag{16b}$$

According to the Rayleigh–Ritz method, the kinematic boundary conditions (16a) must be satisfied, while the static conditions (16b) can be violated. Therefore, a solution is sought representing displacements in double Fourier series

$$u = \sum_{m,n} U_{mn} \cos\frac{m\pi x}{a} \sin\frac{n\pi y}{b}, \quad v = \sum_{m,n} V_{mn} \sin\frac{m\pi x}{a} \cos\frac{n\pi y}{b}, \quad w = \sum_{m,n} W_{mn} \sin\frac{m\pi x}{a} \sin\frac{n\pi y}{b}. \tag{17}$$

Thermal contributions to the stress resultants and stress couples can often be represented by

$$\left\{ N_x^T, \ \ N_y^T, \ \ M_x^T, \ \ M_y^T \right\} = \sum_{mn} \left\{ N_{xmn}, \ \ N_{ymn}, \ \ M_{xmn}, \ \ M_{ymn} \right\} \sin\frac{m\pi x}{a} \sin\frac{n\pi y}{b}. \tag{18}$$

Then the static boundary conditions (16b) are identically satisfied.

The substitution of (17) in (15) yields the potential energy that combines quadratic and linear functions of the amplitudes of displacements:

$$\Pi = \Pi_2 + \Pi_1, \tag{19}$$

where

$$\begin{aligned} \Pi_2 &= \frac{1}{2} \sum_{rs} \sum_{mn} \big(F_{rsmn} U_{rs} U_{mn} + K_{rsmn} V_{rs} V_{mn} + L_{rsmn} U_{rs} V_{mn} + M_{rsmn} U_{rs} W_{mn} \\ &\quad + N_{rsmn} V_{rs} W_{mn} + P_{rsmn} W_{rs} W_{mn} \big) - \frac{1}{2} \sum_{rs} \sum_{mn} T_{rsmn} W_{rs} W_{mn}, \\ \Pi_1 &= \sum_{mn} \{ \tilde{N}^T_{xmn} U_{mn} + \tilde{N}^T_{ymn} V_{mn} - \tilde{M}^T_{mn} W_{mn} \}. \end{aligned} \tag{20}$$

The last term in the expression for Π_2 explicitly depends on the temperature; this term can easily be traced to classical thermal buckling problems.

The "generalized stiffness" coefficients in the first (quadratic) expression of (20) are given by

$$\begin{aligned} F_{rsmn} &= \int_0^a \int_0^b \Big[A_{11}(x, y) \frac{r\pi}{a} \frac{m\pi}{a} S_{rsmn}(x, y) + A_{66}(x, y) \frac{s\pi}{b} \frac{n\pi}{b} C_{rsmn}(x, y) \Big] \mathrm{d}y\, \mathrm{d}x, \\ K_{rsmn} &= \int_0^a \int_0^b \Big[A_{22}(x, y) \frac{s\pi}{b} \frac{n\pi}{b} S_{rsmn}(x, y) + A_{66}(x, y) \frac{r\pi}{a} \frac{m\pi}{a} C_{rsmn}(x, y) \Big] \mathrm{d}y\, \mathrm{d}x, \\ L_{rsmn} &= 2 \int_0^a \int_0^b \Big[A_{12}(x, y) \frac{r\pi}{a} \frac{n\pi}{b} S_{rsmn}(x, y) + A_{66}(x, y) \frac{s\pi}{b} \frac{m\pi}{a} C_{rsmn}(x, y) \Big] \mathrm{d}y\, \mathrm{d}x, \end{aligned}$$

$$M_{rsmn} = -2\int_0^a \int_0^b \left\{ \begin{array}{l} \left[B_{11}(x,y)\left(\frac{m\pi}{a}\right)^2 + B_{12}(x,y)\left(\frac{n\pi}{b}\right)^2\right]\frac{r\pi}{a}S_{rsmn}(x,y) + \\ 2B_{66}(x,y)\frac{s\pi}{b}\frac{n\pi}{b}\frac{m\pi}{a}C_{rsmn}(x,y) \end{array} \right\} \mathrm{d}y\,\mathrm{d}x, \tag{21}$$

$$N_{rsmn} = -2\int_0^a \int_0^b \left\{ \begin{array}{l} \left[B_{22}(x,y)\left(\frac{n\pi}{b}\right)^2 + B_{12}(x,y)\left(\frac{m\pi}{a}\right)^2\right]\frac{s\pi}{b}S_{rsmn}(x,y) + \\ 2B_{66}(x,y)\frac{r\pi}{a}\frac{m\pi}{a}\frac{n\pi}{b}C_{rsmn}(x,y) \end{array} \right\} \mathrm{d}y\,\mathrm{d}x,$$

$$P_{rsmn} = \int_0^a \int_0^b \left\{ \begin{array}{l} \left[D_{11}(x,y)\left(\frac{r\pi}{a}\right)^2\left(\frac{m\pi}{a}\right)^2 + 2D_{12}(x,y)\left(\frac{r\pi}{a}\right)^2\left(\frac{n\pi}{b}\right)^2 + D_{22}(x,y)\left(\frac{s\pi}{b}\right)^2\left(\frac{n\pi}{b}\right)^2\right] \\ \times S_{rsmn}(x,y) + 4D_{66}(x,y)\frac{r\pi}{a}\frac{m\pi}{a}\frac{s\pi}{b}\frac{n\pi}{b}C_{rsmn}(x,y) \end{array} \right\} \mathrm{d}y\,\mathrm{d}x,$$

$$T_{rsmn} = \int_0^a \int_0^b \left[N_x^T(x,y)\frac{r\pi}{a}\frac{m\pi}{a}c_{rx}c_{mx}s_{sy}s_{ny} + N_y^T(x,y)\frac{s\pi}{b}\frac{n\pi}{b}s_{rx}s_{mx}c_{sy}c_{ny}\right]\mathrm{d}y\,\mathrm{d}x,$$

where

$$S_{rsmn}(x,y) = \sin\frac{r\pi x}{a}\sin\frac{s\pi y}{b}\sin\frac{m\pi x}{a}\sin\frac{n\pi y}{b}, \quad C_{rsmn}(x,y) = \cos\frac{r\pi x}{a}\cos\frac{s\pi y}{b}\cos\frac{m\pi x}{a}\cos\frac{n\pi y}{b},$$

$$c_{ix} = \cos\frac{i\pi x}{a}, \qquad s_{ix} = \sin\frac{i\pi x}{a}, \tag{22}$$

$$c_{jy} = \cos\frac{j\pi y}{b}, \qquad s_{jy} = \sin\frac{j\pi y}{b}.$$

The "thermal coefficients" in the second equation of Eq. 20 are

$$\tilde{N}_{xmn}^T = \int_0^a \int_0^b N_x^T(x,y)\frac{m\pi}{a}s_{mx}s_{ny}\mathrm{d}y\,\mathrm{d}x, \quad \tilde{N}_{ymn}^T = \int_0^a \int_0^b N_y^T(x,y)\frac{n\pi}{b}s_{mx}s_{ny}\mathrm{d}y\,\mathrm{d}x,$$

$$\tilde{M}_{mn}^T = \int_0^a \int_0^b \left[M_x^T(x,y)\left(\frac{m\pi}{a}\right)^2 + M_y^T(x,y)\left(\frac{n\pi}{b}\right)^2\right]s_{mx}s_{ny}\mathrm{d}y\,\mathrm{d}x. \tag{23}$$

The Rayleigh–Ritz method yields a system of 3 k coupled linear algebraic equations with respect to the displacement amplitudes in (17), where k is the number of terms retained in these series. In particular, the equations

$$\frac{\partial\Pi}{\partial U_{mn}} = \frac{\partial\Pi}{\partial V_{mn}} = \frac{\partial\Pi}{\partial W_{mn}} = 0 \tag{24}$$

yield

$$\sum_{rs}(F_{rsmn}U_{rs} + L_{mnrs}V_{rs} + M_{mnrs}W_{rs}) + \tilde{N}_{xmn}^T = 0,$$

$$\sum_{rs}(L_{rsmn}U_{rs} + K_{rsmn}V_{rs} + N_{mnrs}W_{rs}) + \tilde{N}_{ymn}^T = 0, \tag{25}$$

$$\sum_{rs}[M_{rsmn}U_{rs} + N_{rsmn}V_{rs} + (P_{rsmn} - T_{rsmn})W_{rs}] - \tilde{M}_{mn}^T = 0.$$

It is noted that the matrix of coefficients at the amplitudes of displacements in (25) is symmetric.

2.4 Exact solution for a thin large-aspect-ratio panel with a piece-wise in-plane constant grading subject to an in-plane uniform thermal load (linear problem)

An exact solution is available in the particular case of a thin large-aspect-ratio piece-wise in-plane graded panel subject to in-plane uniform thermal load as shown in Fig. 3. The analysis of such panels can be conducted by assuming cylindrical bending, i.e., the derivatives of the displacements, strains and stresses with respect to the y-coordinate at a sufficient distance from the short edges are negligible (although the stresses σ_y are present). The heat flow across the boundaries between the regions of a piece-wise constant in-plane grading can be neglected

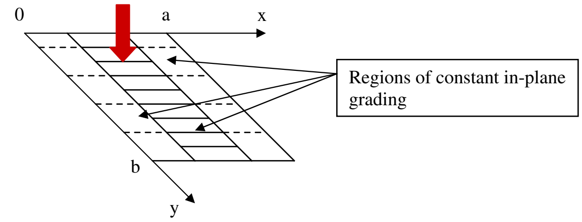

Fig. 3 A large aspect ratio FGM panel with piece-wise constant in-plane grading subjected to thermal loading. The number of regions with in-plane constant grading, their location and the mode of grading may vary

due to heat convection and radiation from the surfaces. Therefore, it is possible to disregard the variations of the thermal contributions to the stress resultants and stress couples within each region of a constant in-plane grading. One can also assume that the elements of the stiffness matrix are constant within each region, even if the effect of the temperature on the material properties is accounted for. Under such an assumption, the solution within the ith region is obtained from the equilibrium equations in displacements available from (3) and (5):

$$A_{11}^{(i)} u_{,xx} - B_{11}^{(i)} w_{,xxx} = 0, \quad D_{11}^{(i)} w_{,xxxx} - B_{11}^{(i)} u_{,xxx} + N_{xi}^{T} w_{,xx} = 0. \tag{26}$$

The solution of (26) is

$$\begin{aligned} w_i &= C_1^{(i)} \cos \beta_i x + C_2^{(i)} \sin \beta_i x + C_3^{(i)} x + C_4^{(i)}, \\ u_i &= C_5^{(i)} x + C_6^{(i)} + \frac{B_{11}}{A_{11}} w_{i,x}, \quad \beta_i = \sqrt{\frac{N_{xi}^T}{D_{11}^{(i)} - B^{(i)}{}_{11}^{2}/A^{(i)}{}_{11}}}, \end{aligned} \tag{27}$$

where the constants of integration are denoted by $C_j^{(i)}$.

The solution must satisfy the continuity conditions between the adjacent ith and $(i+1)$st regions:

$$\begin{aligned} &u_i = u_{i+1}, \quad w_i = w_{i+1}, \quad w_{i,x} = w_{(i+1),x}, \\ &N_{xi} = N_{x(i+1)}, \quad M_{xi} = M_{x(i+1)}, \quad M_{xi,x} - N_{xi}^T w_{i,x} = M_{x(i+1),x} - N_{x(i+1)}^T w_{(i+1),x}. \end{aligned} \tag{28}$$

The last of Eq. 28 reflects the continuity of the transverse shear-stress resultants. The boundary conditions for $x = 0$ and $x = a$ that must be satisfied are the same as in (6), except for the condition $v = 0$ or $N_{xy} = 0$ that is not applicable in case of cylindrical bending.

The number of boundary conditions at the edges, i.e., three conditions at $x = 0$ and at $x = a$, and 6 continuity conditions at each interregional boundary equals the total number of constants of integration. Therefore, the problem is statically determinate. The response mode corresponds to bending since the continuity conditions for the in-plane stress resultants and for the stress couples are nonhomogeneous.

2.5 Example problem: the response of a large-aspect-ratio functionally graded panel to a uniform thermal load applied at the surface

A peculiarity in the response of spatially tailored panels described above is demonstrated here for a relatively simple example of a large-aspect-ratio FGM plate graded exclusively in the thickness direction and subject to a thermal load producing a temperature $T = T(z)$.

2.5.1 Case 1: In-plane boundary condition $N_x = 0$ (at both ends)

The solution is available using the results of Sect. 2.4 in the form

$$u_{,x} = \frac{B_{11}}{A_{11}} w_{,xx} + \frac{N_x^T}{A_{11}}, \quad w = C_1 \cos \beta x + C_2 \sin \beta x + C_3 x + C_4, \quad \beta = \sqrt{\frac{N_x^T}{D_{11} - B_{11}^2/A_{11}}}. \tag{29}$$

Case 1a: Clamped panel. In this case, the constants of integration are found from the following system of homogeneous equations:

$$\begin{bmatrix} 1 & 0 & 0 & 1 \\ 0 & \beta & 1 & 0 \\ \cos\beta a & \sin\beta a & a & 1 \\ -\beta\sin\beta a & \beta\cos\beta a & 1 & 0 \end{bmatrix} \begin{Bmatrix} C_1 \\ C_2 \\ C_3 \\ C_4 \end{Bmatrix} = 0. \tag{30}$$

It is obvious that prebuckling deformations involve only in-plane displacements, without bending. The critical thermal load can be found from the requirement of a nonzero solution of the system of equations (30). The panel buckles and subsequently develops postbuckling bending deformations in response to an additional load. Note that such a response occurs in spite of the fact that the in-plane boundary conditions include a thermal term, since $u,_x$ does not affect the buckling equation available from (30).

Case 1b: Simply supported panel. The boundary conditions yield a nonhomogeneous system of equations with respect to the constants of integration in (29):

$$\begin{bmatrix} 1 & 0 & 0 & 1 \\ 1 & 0 & 0 & 0 \\ \cos\beta a & \sin\beta a & a & 1 \\ \cos\beta a & \sin\beta a & 0 & 0 \end{bmatrix} \begin{Bmatrix} C_1 \\ C_2 \\ C_3 \\ C_4 \end{Bmatrix} = \frac{M_x^T - N_x^T/A_{11}}{\left(D_{11} - B_{11}^2/A_{11}\right)\beta^2} \begin{Bmatrix} 0 \\ 1 \\ 0 \\ 1 \end{Bmatrix}. \tag{31}$$

Having found the constants of integration from (31), one can determine the primary bending load-deformation path.

The load that causes instability of the primary bending path is found as follows. The variations in the stress resultant and stress couple including the terms associated with prebuckling bending deformations (these terms are underlined) and neglecting nonlinear variational terms are

$$\delta N_x = A_{11}\left(\delta u,_x + \underline{w,_x \delta w,_x}\right) - B_{11}\delta w,_{xx}, \quad \delta M_x = B_{11}\left(\delta u,_x + \underline{w,_x \delta w,_x}\right) - D_{11}\delta w,_{xx}. \tag{32}$$

The substitution of (32) in the variational equilibrium equations available from (9) yields a system of homogeneous equations with respect to δu, δw and their derivatives:

$$\begin{aligned} &A_{11}(\delta u,_{xx} + \underline{w,_x \delta w,_{xx} + w,_{xx}\delta w,_x}) - B_{11}\delta w,_{xx} = 0, \\ &D_{11}\delta w,_{xxxx} - B_{11}\delta u,_{xxx} - \underline{B_{11}\left(w,_x \delta w,_{xxx} + 2w,_{xx}\delta w,_{xx} + w,_{xxx}\delta w,_x\right)} + N_x \delta w,_{xx} \\ &\quad + w,_{xx}\left[A_{11}\left(\delta u,_x + \underline{\underline{w,_x \delta w,_x}}\right) - B_{11}\delta w,_{xx}\right] = 0, \end{aligned} \tag{33}$$

where N_x includes both prebuckling deformations as well as the thermal contribution, i.e.,

$$N_x = \underline{A_{11}u,_x - B_{11}w,_{xx}} - N_x^T. \tag{34}$$

The doubly underlined term in (33) is nonlinear with respect to prebuckling deformations and can be neglected.

The analysis neglecting prebuckling deformations can be conducted by omitting the underlined terms in (33) and (34). However, prebuckling bending may be considerable and such a simplification is not recommended.

The variational boundary conditions $\delta w = \delta M_x = \delta N_x = 0$ being homogeneous, the buckling thermal load can be determined from the nonzero requirement to the variations δu and δw in (33). The postbuckling load-deformation path can be determined by adding a geometrically nonlinear term $\frac{1}{2}\delta w,_x^2$ to the variation of the axial strain in the expressions for the stress resultant and couple (32) and accounting for additional thermal load, in excess of the buckling load. As a result, the variational equilibrium equations and boundary conditions become nonlinear with respect to the displacements counted from the prebuckling state and the postbuckling load-deformation path can be evaluated.

2.5.2 *Case 2: In-plane boundary condition $u = 0$ (at both ends)*

In addition to the deflection w given by (29), the first equation of equilibrium, i.e., $N_x,_x = 0$ yields

$$u = C_5 x + C_6 + \frac{B_{11}}{A_{11}} w,_x \tag{35}$$

Table 1 Layer-wise content of TiB through the thickness of the panel and the properties of layers as functions of the content of TiB

Layer	%TiB FGM	%TiB symmetric	
1	0	85	
2	15	75	
3	30	60	
4	45	45	
5	60	60	
6	75	75	
7	85	85	
%TiB	E (GPa)	ν	CTE*10^6 (1/C)
0	107	0.34	8.6
15	121	0.31	8.39
30	133	0.28	8.17
45	159	0.25	7.96
60	193	0.22	7.72
75	237	0.19	7.51
85	274	0.17	7.36

E = modulus of elasticity, ν = Poisson's ratio, CTE = coefficient of thermal expansion
"FGM" = distribution of seven layers through the thickness (Figs. 5, 6), "symmetric" = distribution of layers in the central part of the panel in Fig. 6

Obviously, the boundary conditions $u = 0$ applied at both ends yield two homogeneous equations with respect to the constants of integration.

Case 2a: Clamped panel. Equations (30) jointly with the conditions $u = 0$ result in a system of six homogeneous algebraic equations with respect to the constants of integration. Obviously, the panel will buckle without developing prebuckling bending deformations. The postbuckling behavior of such panels can be conducted using the approach similar to that discussed in [22].

Case 2b: Simply supported panel. In such a panel the boundary condition $M_x = 0$ is nonhomogeneous. As a result, the panel experiences bending that increases with the load, i.e., its behavior is characterized by Fig. 2a.

2.6 Example: distribution of postbuckling stresses in a Ti/TiB panel with an initial imperfection subject to a uniform temperature

An illustration of the effectiveness of spatially tailored and functionally graded materials is presented in this section for a panel composed of titanium (Ti) and titanium boride (TiB). The panel is 0.846 m long and 0.282 m wide. The thickness of the panel composed of seven layers is 2.8 mm. Each layer is 0.4 mm thick; the properties of the layers are shown in Table 1. The long edges of the panel are simply supported and prevented from out-of-plane displacements, i.e., $u = v = w = 0$, while the short edges are free.

The panels considered in the example have an initial imperfection corresponding to the buckling-mode shape with an amplitude equal to 0.7 mm. The maximum (in terms of the absolute value) in-plane principal stresses generated by a uniform temperature of 150°C and calculated by ABAQUS are shown for the following cases:

– Titanium panel without added titanium boride (Fig. 4);
– FGM panel graded in the thickness direction according to Table 1 (Fig. 5);
– Space-tailored panel consisting of FGM sections and a central strip that is 0.0846 m wide where seven Ti/TiB layers are symmetrically arranged about the middle plane (Fig. 6).

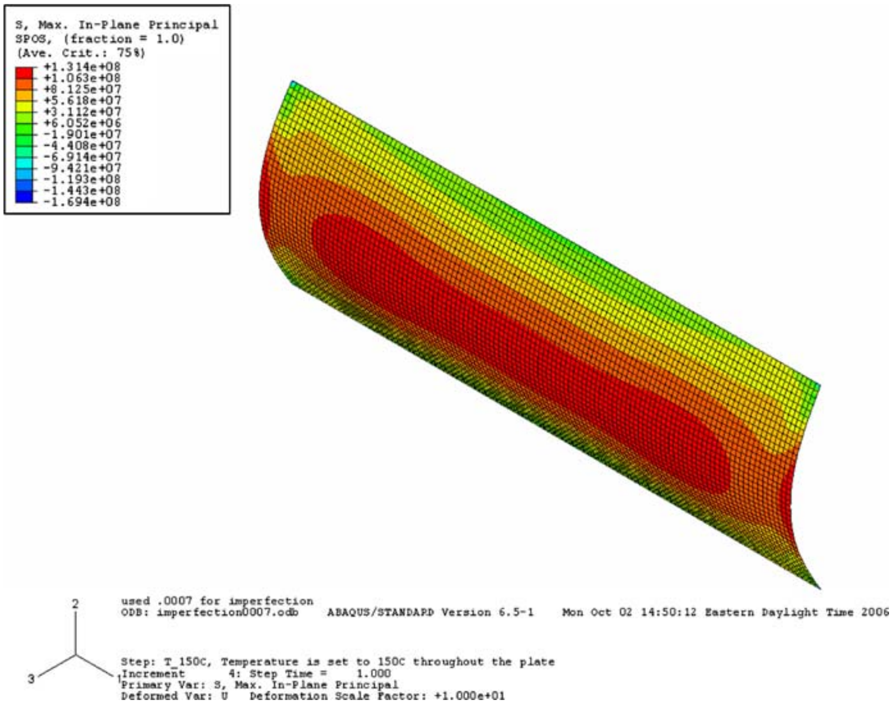

Fig. 4 Maximum in-plane principal stresses in a titanium panel as a result of $T = 150°\mathrm{C}$

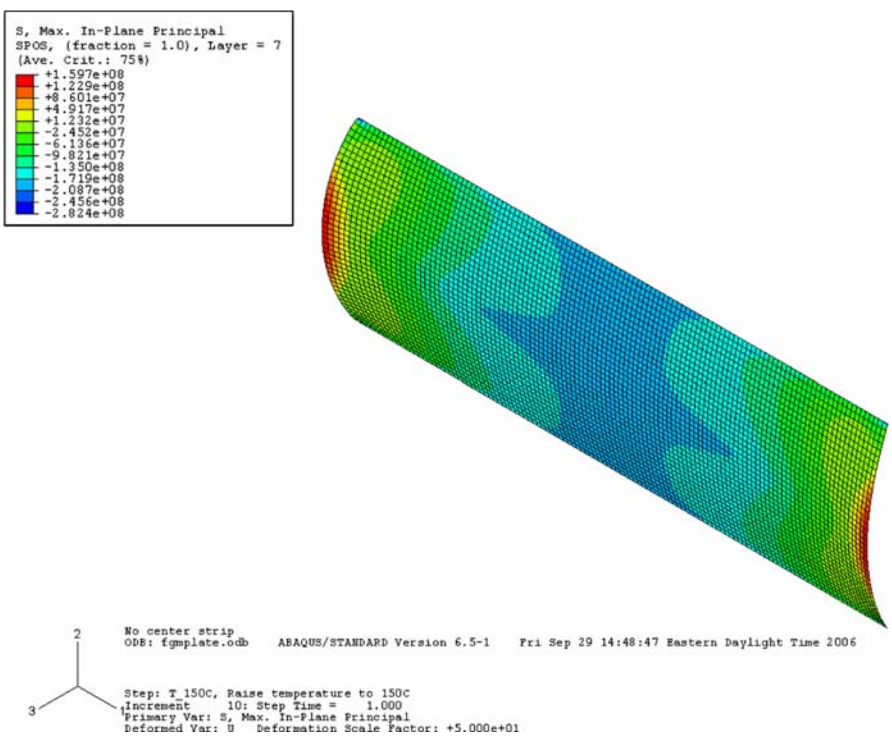

Fig. 5 Maximum in-plane principal stresses in a FGM Ti/TiB panel as a result of $T = 150°\mathrm{C}$

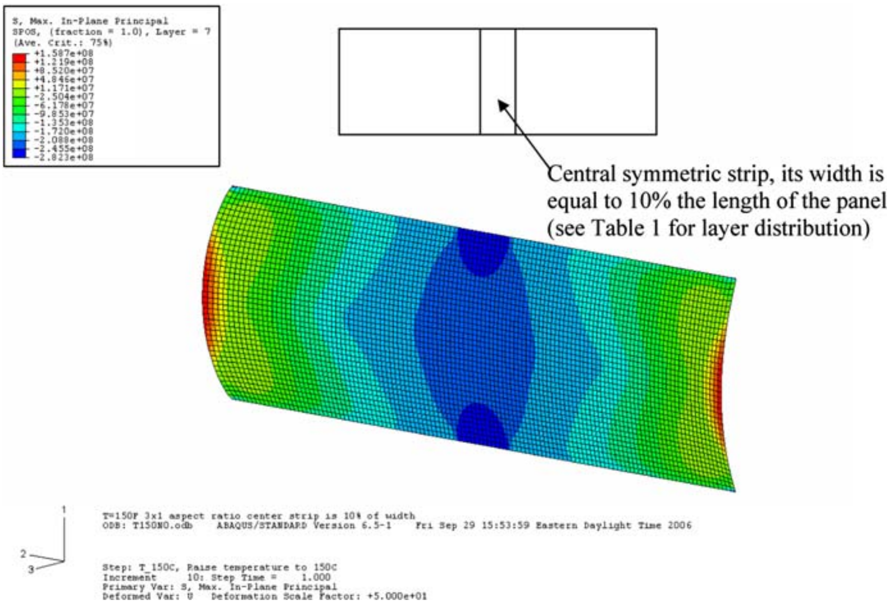

Fig. 6 Maximum in-plane principal stresses in a FGM Ti/TiB panel with a central symmetric strip as a result of $T = 150°\text{C}$

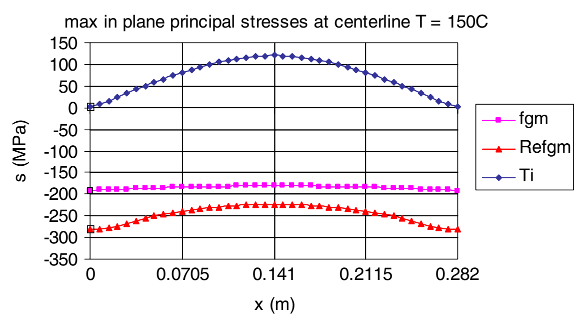

Fig. 7 Maximum in-plane principal stresses at the centerline of the panel as a result of $T = 150°\text{C}$. Legend: fgm = FGM panel, Refgm = FGM panel with a central symmetric strip, Ti = titanium panel

As follows from Figs. 4–6, grading can alter the maximum principal stresses from tensile in a titanium panel to compressive in a FGM panel. The addition of a symmetric strip in the central section of an FGM panel further increases the compressive principal stresses. A comparison between the distributions of the maximum principal stresses along the centerline of the panel is presented in Fig. 7. The stresses at the edges of the panel are not actually equal to zero as may look likely in Fig. 7, but they are quite small and do not show in the scale used this figure. As follows from this figure, using functionally graded materials and, in particular, using space-tailored panels represents a powerful tool for modifying and/or optimizing the response of a panel to thermal loading. For example, changing the principal stresses from tension to compression achieved in FGM and spatially tailored panels may prevent or arrest cracks in the panel. Note that all stresses in Figs. 4–7 remain within the elastic range. A higher temperature could result in plastic effects and creep that are not considered in the present model.

3 Conclusions

We have outlined an approach to the stress and deformation analysis of a class of spatially tailored advanced thermal structures (STATs) represented by rectangular panels with three- or two-dimensional arbitrary grading in the direction of the coordinate axes. The applied thermal load and the resulting temperature distribution throughout the panel can be arbitrary. The effect of temperature on the local material properties can be incorporated in the analysis. The Rayleigh–Ritz solution is illustrated for the case where the edges of the panel are simply supported. An exact solution has been presented for a thin large-aspect-ratio panel composed of strips of in-plane constant grading oriented along the long edges. An example of the response of large-aspect-ratio panels graded in the thickness direction and subject to thermal-loading-producing temperature that varies in the same direction has been considered. The difference in the response affected by the boundary conditions was illustrated by this example.

The following conclusions can be drawn from the analysis of the governing equations for various cases of grading:

1. Panels with in-plane grading characterized by arbitrary continuous functions or by piece-wise constant functions of in-plane coordinates respond to arbitrary thermal loading by bending from the equilibrium position. As the thermal load increases, the panel can fail due to the loss of strength. Alternatively, the primary equilibrium bending path may become unstable. In this case the panel switches to a new load-deformation path without an abrupt snap-through that is typical for shell structures.
2. An exception to the behavior of continuously or piece-wise in-plane graded panels described above is found in an unlikely case where thermal stress couples and stress resultants are constant throughout the panel if the boundary conditions correspond to those specified in (11). Such panels do not experience prebuckling bending; they buckle and develop postbuckling deformations as the load increases.
3. Panels graded exclusively in the thickness direction and subjected to thermal loading develop bending deformations in response to this loading (a subsequent buckling is possible, as is shown in Fig. 2a). An exception is found in panels with boundary conditions (11) subject to thermal loading that is uniformly distributed over the exposed surface. These panels do not develop prebuckling bending deformations. Instead, they buckle at a critical load and exhibit postbuckling deformations as the load continues to increase.
4. Large-aspect-ratio FGM panels graded in the thickness direction and subject to a uniform thermal load (heat flux or elevated temperature) applied at a surface experience prebuckling bending if the long edges are simply supported and buckling without previous bending if they are clamped.
5. The use of functionally graded or space-tailored materials may alter the thermal stresses within a panel, including changing the sign of the maximum principal stress. This offers numerous opportunities open to an engineer incorporating such materials in design.

Acknowledgements This research was sponsored by the Structural Sciences Center/Air Vehicles Directorate/Air Force Research Laboratory through the contract GS-23F8049H (F33601-03-F-0060).

References

1. Birman V, Byrd LW (in press) Modeling and analysis of functionally graded materials and structures. Appl Mech Rev
2. Tsukamoto H (2003) Analytical method of inelastic thermal stresses in a functionally graded material plate by a combination of micro- and macromechanical approaches. Compos Part B: Eng 34:561–568
3. Ootao Y, Tanigawa Y (1999) Three-dimensional transient thermal stresses of functionally graded rectangular plate due to partial heating. J Thermal Stresses 22:35–55
4. Ootao Y, Tanigawa Y (2004) Transient thermoelastic problem of functionally graded thick strip due to nonuniform heat supply. Compos Struct 63:139–146
5. Reddy JN, Cheng Z-Q (2001) Three-dimensional thermomechanical deformations of functionally graded rectangular plates. Eur J Mech Ser A/Solids 20:841–855
6. Reddy JN, Chen CD (1998) Thermomechanical analysis of functionally graded cylinders and plates. J Thermal Stresses 21:593–626
7. Praveen GN, Reddy JN (1998) Nonlinear transient thermoelastic analysis of functionally graded ceramic-metal plates. Int J Solids Struct 35:4457–4476
8. Vel SS, Batra RC (2002) Exact solution for thermoelastic deformations of functionally graded thick rectangular plates. AIAA J 40:1421–1433
9. Vel SS, Batra RC (2003) Three-dimensional analysis of transient thermal stresses in functionally graded plates. Int J Solids Struct 40:7181–7196
10. Qian LF, Batra RC (2004) Transient thermoelastic deformations of a thick functionally graded plate. J Thermal Stresses 27:705–740
11. Yang J, Shen H-S (2003) Nonlinear bending analysis of shear deformable functionally graded plates subjected to thermo-mechanical loads under various boundary conditions. Compos Part B: Eng 34:103–115

12. Javaheri R, Eslami MR (2002) Thermoelastic buckling of rectangular plates made of functionally graded materials. AIAA J 40: 162–169
13. Javaheri R, Eslami MR (2002) Thermal buckling of functionally graded plates based on higher-order theory. J Thermal Stresses 25:603–625
14. Na K-S, Kim J-H (2004) Three-dimensional thermal buckling analysis of functionally graded materials. Compos Part B: Eng 35:429–437
15. Na K-S, Kim J-H (2006) Three-dimensional thermomechanical buckling analysis for functionally graded composite plates. Compos Struct 73:413–422
16. Na K-S, Kim J-H (2006) Thermal postbuckling investigations of functionally graded plates using 3-D finite element method. Finite Elements Anal Design 42:749–756
17. Ganapathi M, Prakash T (2006) Thermal buckling of simply supported functionally graded skew plates. Compos Struct 74:247–250
18. Birman V, Chona R, Byrd LW (2006) Effect of two-dimensional grading on the thermomechanical response of the panel. In: Paulino GH, Pindera M-J, Dodds RH, Rochinha FA (eds) *Proceedings of FGM 2006:* multiscale & functionally graded materials conference, Honolulu, Hawaii, October 2006 (in press)
19. Mills AF (1995) Basic heat and mass transfer. Irwin, Chicago
20. Reddy JN (2004) Mechanics of laminated and composite plates and shells. Theory and analysis. CRC Press, Boca Raton, pp 126–127
21. Tauchert TR (1995) Temperature and absorbed moisture. In: Turvey GJ, Marshall IH (eds) Buckling and postbuckling of composite plates. Chapman & Hall, London pp 190–226
22. Birman V (2005) Thermally induced bending and wrinkling in large aspect ratio sandwich panels. Compos Part A: Appl Sci Manufact 36:1412–1420